doi:10.2533/chimia.2018.614 Chimia 72 (2018) 614–620

Selectivity in Transition Metal-catalyzed Cyclizations: Insights from Experiment and Theory

Edward A. Anderson*[a] and Robert S. Paton[b]

Abstract: Transition metal-catalyzed cycloisomerization reactions offer a powerful tool for the synthesis of complex cyclic organic molecules from acyclic precursors. In addition to ring formation, these processes can result in the generation of new stereocentres at the site of ring formation; understanding the origins of stereoselectivity enables the use of cycloisomerization chemistry in synthesis, and promotes the design of new reactions. In this article, some recent developments from our groups in regio- and stereoselective cycloisomerization reactions are discussed. Alongside experimental observations, crucial to developing a robust understanding of selectivity has been the use of computation to explore theoretical reaction pathways, which provides an exceptional level of insight into selectivity. In its most valuable form, this correlation between experiment and theory enables the design of improved catalyst systems exhibiting both enhanced reactivity, and selectivity.

Keywords: Cycloisomerization · Mechanistic Study · Selectivity · Theoretical analysis · Transition metal catalysis

Edward Anderson did his PhD with Andrew Holmes in Cambridge. Following postdoctoral work with Erik Sorensen at the Scripps Research Institute in La Jolla, Ed returned to Cambridge as a Junior Research Fellow at Homerton College, working with Ian Paterson. In 2007, he took up an EPSRC Advanced Research Fellowship at Oxford, and in 2009 was appointed to a University Lectureship at Jesus College. In 2014 He was appointed as an Associate Professor, and as Professor in 2016. His interests cover the full range of organic chemistry, including asymmetric catalysis, new synthetic methods, natural products, ynamide and organosilicon chemistry, bioisosteres, biosynthesis, and nucleic acids.

Robert Paton obtained his PhD with Jonathan Goodman in Cambridge. Following a Junior Research Fellowship at St Catharine's College, Cambridge, and a period in the group of Feliu Maseras at ICIQ, Rob conducted postdoctoral research with K. N. Houk at UCLA from 2009-2010. In 2010 he was appointed as a University Lecturer at Oxford, and as an Associate Professor in 2014. He is the recipient of the MGMS Silver Jubilee Prize, the RSC Harrison-Meldola Memorial Prize, and an ACS OpenEye Outstanding Junior Faculty Award. In 2018, Rob moved to Colorado State University. His interests span all aspects of computational organic chemistry, in particular understanding catalytic processes, and rationalizing synthesis and biosynthesis.

Introduction

Transition metal-catalyzed cycloisomerizations are among the most efficient means to construct cyclic organic molecules from relatively simple acyclic precursors.[1] These processes are highly attractive to synthetic chemists not only due to their high atom economy, but also the range of different ring architectures that can arise from a given precursor through choice of the catalyst system. Some examples of general reaction classes (Scheme 1) include single component cyclizations (such as enyne cycloisomerization, path a), higher order single component processes (for example, [5+2] cycloisomerizations, path b), two component higher order processes (such as the Pauson-Khand reaction, path c), and multicomponent higher order reactions (exemplified by [2+2+2] cyclotrimerization, path d). Along with this catalyst- and substrate-dependent diversity of product connectivity, exquisite control can also be achieved over the stereochemistry at new stereocentres or double bonds formed during the cyclization, rendering these reactions powerful tools in synthesis. Nonetheless, establishing robust models to explain reaction outcomes – which would enable the confident implementation of cycloisomerization strategies in target-oriented synthesis – is non-trivial due to the potential operation of different reaction pathways. In this article, we discuss three recent examples of transition metal-catalyzed cyclization reactions from our groups, where the combination of theoretical and experimental chemistry provided detailed insight into reaction mechanisms, rationalization of selectivities in product formation, and even facilitated optimization in the design of more reactive and selective catalyst systems. Collectively, these studies illustrate how computational analysis of reaction pathways can not only serve as a tool for post-reaction rationalization, but can also influence reaction design, and offer fresh insight into the fundamental steps of even the most classical of cycloisomerizations.[2]

*Correspondence: Prof. E. A. Anderson
E-mail: edward.anderson@chem.ox.ac.uk
[a]Chemistry Research Laboratory
University of Oxford
12 Mansfield Road, Oxford, OX1 3TA, UK
[b]Department of Chemistry
Colorado State University
Center Avenue, Fort Collins, CO 80523, USA

Palladium-catalyzed Cyclization Reactions of Propargylic Carbonates[3]

Our forays into the combined use of computation and experiment to rationalize selectivity in transition metal-catalyzed transformations began with the palladium-catalyzed synthesis of alkynyl heterocycles (**1**, Scheme 2) from propargylic carbonates (**2**) equipped with internal nucleophiles. This process involves a formal substitution of the carbonate leaving group with overall retention of configuration, due to the high stereochemical fidelity of the initial S_N2' oxidative addition of the substrate (to give an allenylpalladium(II) intermediate **3**),[4] and the subsequent S_N2' reductive elimination by attack of the tethered nucleophile. In the course of reaction optimization, particularly for sulfonamide nucleophiles, an additional product was observed – heterocyclic enamide **4**. Particularly intriguing was that the ratio of alkynyl heterocycle/enamide (1 : 4) appeared to be related to the nature of the bidentate phosphine ligand employed in the reaction: the large bite angle ligand DPEphos (Φ ~ 105°) favoured the formation of **1**, while the small bite angle ligand dppe (Φ ~ 86°) favoured **4**. The bite angle of bidentate phosphine ligands is well-recognized to be an important factor in controlling reaction outcomes,[5] but the reasons for this switch in regioselectivity were not clear. Nonetheless, the ability to control the site of nucleophilic attack on an allenylpalladium complex simply through selection of an appropriate ligand could undoubtedly provide useful synthetic opportunities; it is also notable that this behaviour contrasts with that typically observed in an intermolecular context, in which nucleophiles engage the allenylpalladium intermediate at its central carbon atom.[6]

Allenylpalladium complexes[7] typically exist in equilibrium between η^1-complexes **5** (Scheme 3), which may be neutral or cationic depending on the nature of the ligand, and cationic η^3-complexes **6**,[8] in which the orthogonal 'distal' alkene also coordinates to the metal ion. Theoretical analysis of this more electrophilic η^3 complex enabled rationalization of the observed selectivity, based on the finding that the structure of **6** varies subtly with the extent of complexation of the second alkene. This results in differing degrees of 'bending' of the allene unit; using model complexes (**7** and **8**), we were able to explore the dependence of the calculated angle of allene bend on calculated bidentate ligand bite angle (see inset graph, wB97XD/6-31G(d) level of theory). This revealed a more significant distortion from linearity of the allenylpalladium geometry for smaller bite angle ligands, correlating with stronger binding of the metal to the distal alkene of the allenylpalladium complex. Greater complexation in turn raises the energy of the Pd–C antibonding orbital (calculations at the wB97XD/def2-TZVPP level of theory), disfavouring attack at the remote carbon atom, with reaction at the central carbon atom thus being observed. However, as the ligand bite angle increases, the allene geometry becomes more linear, and the Pd–C bond to the distal carbon atom lengthens. This weakens metal–carbon bonding at this site, lowering the energy of the LUMO (which has a non-zero coefficient at this position) and rendering this carbon atom more susceptible to nucleophilic attack – leading to the alkynyl heterocycle product. Interestingly, the charge distribution across these atoms varies little between these structures, ruling out a purely electrostatic explanation. Overall, the experimentally observed change in regioselectivity for these two complexes can thus be explained by stereoelectronic effects arising from the geometric influence of the ligands.

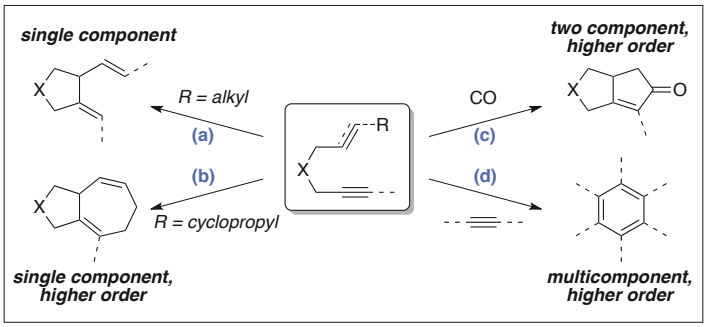

Scheme 1. General examples of transition metal-catalyzed cycloisomerization.

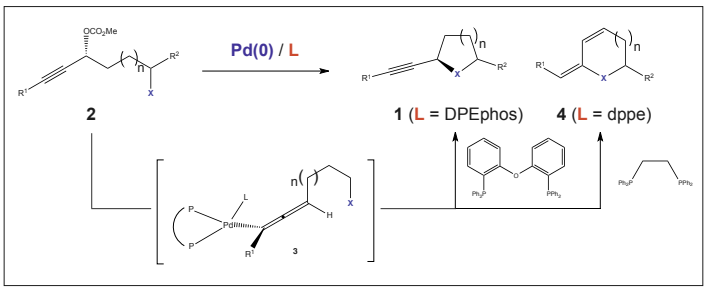

Scheme 2. Ligand-dependent regioselective palladium-catalyzed cyclization reactions of propargylic carbonates.

Palladium(II) Acetate-catalyzed Cycloisomerization Reactions of Enynamides and Enynes[9]

Within the field of cycloisomerization chemistry, palladium-catalyzed enyne cycloisomerizations (of general form **9**→**10/11**, Scheme 4a) are among the most well-established, with this chemistry originating in the groundbreaking publications by Trost in the 1980s[10] and early 1990s.[11] A number of relatively simple catalyst systems are available, including palladium(0) pre-catalysts (*e.g.* Pd_2dba_3/AcOH, with or without phosphine ligand) and palladium(II) complexes (*e.g.* $Pd(OAc)_2/PPh_3$). Our own interest in this field stemmed from various applications of enynamides in ring-forming reactions,[12] as enynamide cycloisomerization offers an attractive and atom-economical entry to azacycles. We discovered that enynamides **9** (X = CH_2, Y = NTs) are indeed excellent substrates for this chemistry; some example products are shown (Scheme 4b), in which efficient formation of various azacycles, including bicyclic products, could be achieved using $Pd(OAc)_2$ in combination with the ligand *bis*-benzylidene ethylenediamine (bbeda). Of particular appeal to us was the installation of, and control over, new stereocentres in the course of ring formation, where very high levels of substrate stereocontrol were observed. This piqued our interest in the mechanism of the cyclization, an understanding of which would provide a platform for the wider use of this chemistry in synthetic contexts.

Historically, the mechanism by which these palladium-catalyzed cycloisomerizations proceed has been the source of much debate. Due in part to contrasting reaction outcomes and product distributions, Trost originally proposed two distinct pathways to operate from Pd(0) and Pd(II) precatalysts (Scheme 4c). For the former, in the presence of acetic acid, a rapid and reversible oxidative addition of Pd(0) into the carboxylic acid O–H bond was proposed to afford a palladium(II) hydride species, which would then undergo migratory insertion of first the alkyne component (hydropalladation), and then the alkene component (ring-forming carbopalladation), with a final β-hydride elimination affording product. In contrast, Pd(II) catalysts were first proposed to undergo an oxidative coupling with the Pd(II)-complexed enyne, leading

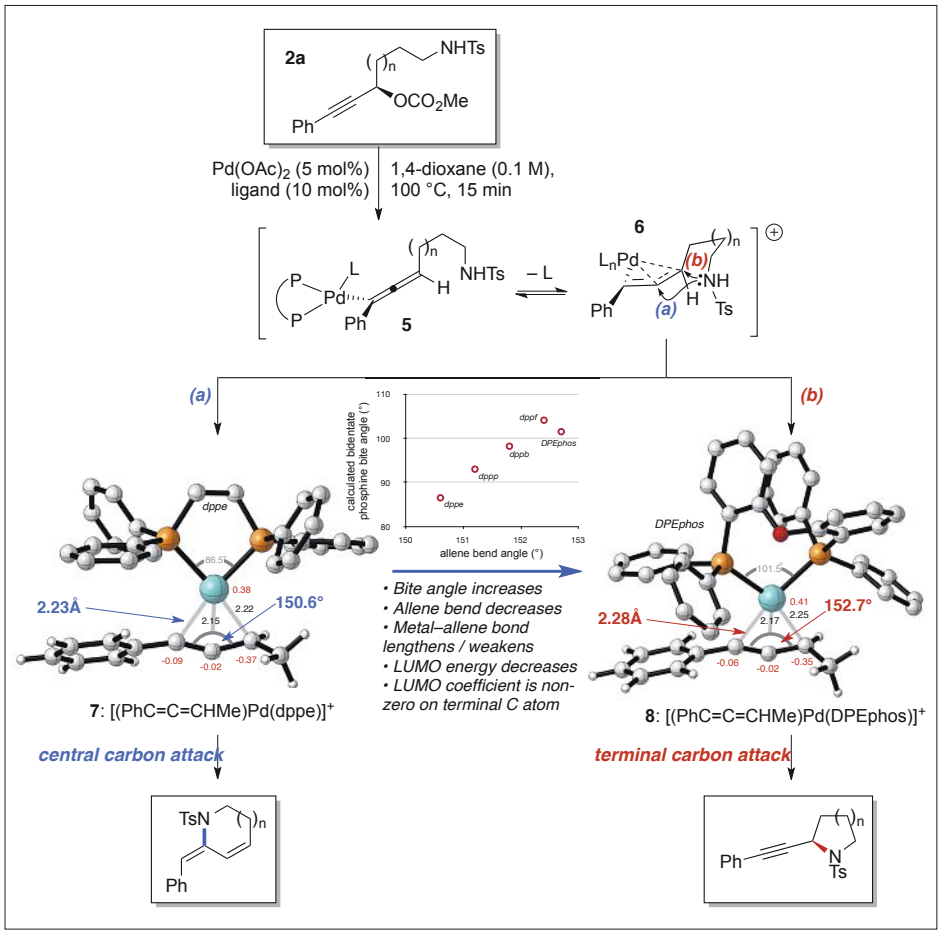

Scheme 3. Computational rationalization of regioselectivity profiles reveal a stereoelectronic influence of ligand bite angle on allenylpalladium reactivity.

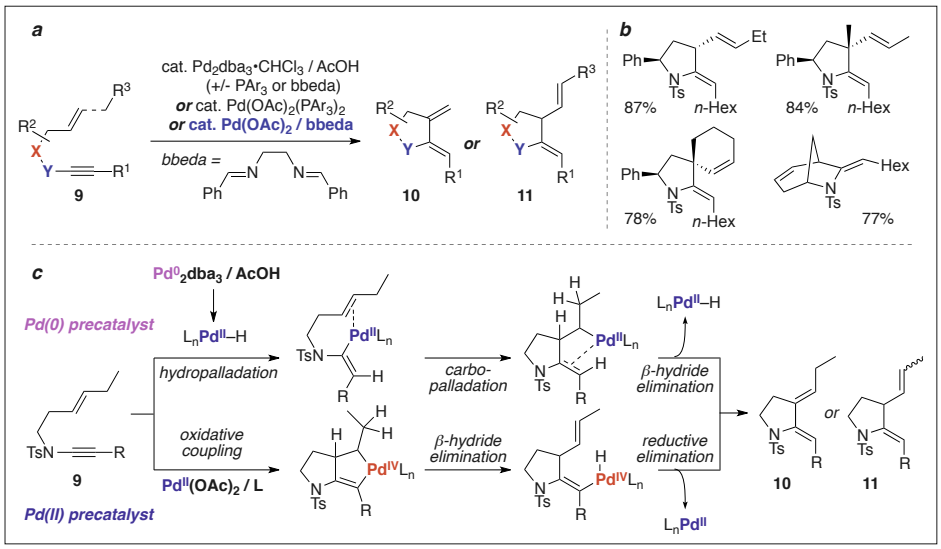

Scheme 4. a) Palladium-catalyzed enyne and enynamide cycloisomerization; b) examples of enamide products; and c) mechanistic possibilities.

to a palladium(IV) palladacyclopentene intermediate. β-Hydride elimination would deliver an alkenylpalladium hydride, with reductive elimination giving the diene product. Support for the intermediacy of a Pd(IV) palladacycle, which is key to this mechanism, was found in the characterization (and indeed use as a precatalyst) of various palladacyclopentadiene complexes; however, no examples of palladacyclopentenes are yet known. In the context of our own work, we questioned whether enynamides could be used to probe which pathway, if either, was operable under $Pd(OAc)_2$/bbeda catalysis.

Our studies initially focused on deuterium labelling experiments where, under both Pd_2dba_3 and $Pd(OAc)_2$ catalysis, equal proportions of deuteriated product were observed starting from a 1:1 mixture of enynamides **12** and **D-13**. This is indeed consistent with the formation of discrete Pd(II)–hydride species which effect intermolecular hydropalladation, rather than a metallacycle pathway where retention of H/D within a given substrate would be expected (an outcome reinforced by the complete retention of deuterium in product **D-14** from the equivalent experiment performed using Cp*Ru(cod)Cl, where metallacycle intermediacy is accepted). Independent ^{1}H NMR reaction profiling of **13** and **D-13** revealed several interesting features: first, the rate of cyclization of the deuterated substrate **D-13** was significantly slower than non-deuterated **13**; second, incomplete deuterium transfer was observed in the reactions of **D-13** (~65-80%); third, the *extent* of product deuteriation varied with conversion – at early reaction stages, only non-deuterated product **14** was formed, while at later stages only deuterated product **D-14** was produced; finally, a notable induction period was exhibited in these reactions, which we hypothesized was related to the formation of a catalytically active palladium species.

After some investigations, we determined that H_2O present in the NMR reaction solvent was at least partially responsible for the formation of protiated product **14** over deuteriated product **D-14**. This showed that water could mediate exchange of deuterium for hydrogen on one (or more) of the catalytic intermediates; however, even under rigorously dry reaction conditions (~3 ppm H_2O), and using substrate **D-13** with 100% D at the internal alkene carbon, around 15% of protiated product **14** was still formed (early) in the reaction. The answer to this puzzle, and indeed key insight into the mode of initiation, arose from our realization that small amounts of benzaldehyde were observed by ^{1}H NMR spectroscopy in 'non-dried' reaction solvents. This could only derive from the so-called ligand, bbeda, *via* imine hydrolysis, which led us to speculate that palladium(II) might not only promote this hydrolysis by acting as a Lewis acid, but that the resultant Pd(II)-complexed amine could serve as a source of palladium hydride through β-hydride elimination. Further hydrogen atoms could later be released by imine–enamine tautomerism, thus explaining the ~15% of protiated product **13** observed at 5 mol% bbeda loading. To test this, we prepared backbone perdeuterated d_4-bbeda, and to our delight (Scheme 5c), complete suppression of product protiation was observed using this ligand. Further, a small proportion of deuterated product **D-13** was formed from non-deuterated substrate **12** using d_4-bbeda, a reaction in which the imine is the only possible source of deuterium atoms.

While we now believed we had identified a pathway for reaction initiation, and that a palladium(II) hydride-based mechanism might indeed be involved, we were keen to conduct a theoretical analysis of the reaction mechanism to determine if such a pathway were energetically feasible, and to enable eventual explanation of reaction stereoselectivity. A reaction profile was thus computed (SMD-TPSS-D3/def2-TZVP level of theory) which revealed a number of interesting aspects (Scheme 6). Chief among these was that an enynamide complex of palladium(II)H(OAc) lay >20 kcal mol^{-1} higher in energy than the equivalent enynamide complex with palladium(0)(κ^2-HOAc) (complex A); in other words, at the point of alkyne hydropalladation, the lower oxidation state of the metal was strongly favoured. Importantly, ground state A also progressed *via* a significantly lower energy transition state TS_AB *en route* to alkenylpalladium(II) complex B, whereby the Pd(0) complex directly converts to the Pd(II) product without formation of a discrete palladium(II) hydride intermediate, and in which the hydrogen atom being transferred is simultaneously bonded to acetate, the metal, and the carbon atom – a novel process we termed 'oxidative hydrometallation'. This irreversible process is followed by a second irreversible step – carbopalladation of the alkene to form the cyclic framework (C). Of great interest was that the rate-determining step of the cycloisomerization is β-hydride elimination, where the high energetic cost of this step mainly arises from the penalty of decomplexation of the enamide from the metal to permit C–C bond rotation (C→C'), and thus position the C–Pd bond *syn* with the adjacent C–H bond. Following this step, the resulting palladium(II) hydride D was found to be in a low-barrier equilibrium with palladium(0) acetic acid complex E, providing a reasonable pathway for acid-mediated exchange of deuterium and hydrogen in reactions where extensive product protiation is seen.

That protiated product (*e.g.* **14**) should form in strong preference to deuteriated product (**D-14**) was supported by a significant predicted kinetic isotope effect (kie) for the first (irreversible) hydropalladation. While this kie could not be observed directly (indirect evidence was obtained by off-pathway equilibrium isotope effects, where the overall observed kie for the reaction was found to vary with catalyst concentration), we *were* able to determine experimentally a kie of 2.29 for the turnover-limiting β-hydride elimination, which pleasingly correlated well with the computational prediction of 2.23.

Importantly, this computational model provided an opportunity to explore the diastereoselectivity of the cyclization process (Scheme 7, see also examples in Scheme 2). From an empirical perspective, the high levels of stereocontrol exerted in the cyclization of substrates such as **15** to diastereomers **16**-*anti* are hard to rationalize, as both potential conformers **15**-*syn* and **15**-*anti* seem to exhibit steric interactions that would not favour one ground state over the other. Indeed, computationally, these ground states were found to be of very similar energy (SMD-TPSS-D3/def2-TZVP), with the difference in reactivity instead depending exclusively on the difference in transition state energies for carbopalladation ($\Delta\Delta G^{\ddagger}$ = 3.4 kcal mol^{-1}). Examination of these transition states reveals that this energy difference may relate to the changing conformation of the C–C bond between the alkene undergoing carbopalladation, and the tether (bond indicated in blue). In the case of the lower energy (*anti*) transition state, the alkenyl C–H bond (red) and one of the allylic C–H bonds (green) moves from an eclipsed conformation to a staggered orientation as carbopalladation proceeds, corresponding to a relief of torsional strain. The opposite is true for the disfavoured (*syn*) transition state (red): here, the dihedral angle between these same C–H bonds decreases (towards an eclipsed conformation) as carbopalladation occurs. The observation that changes in torsional strain can affect the stereochemical outcome of a metal-catalyzed process, rather than more classical steric arguments associated based on reactant conformation, offers interesting opportunities for the design of such processes into synthetic contexts.

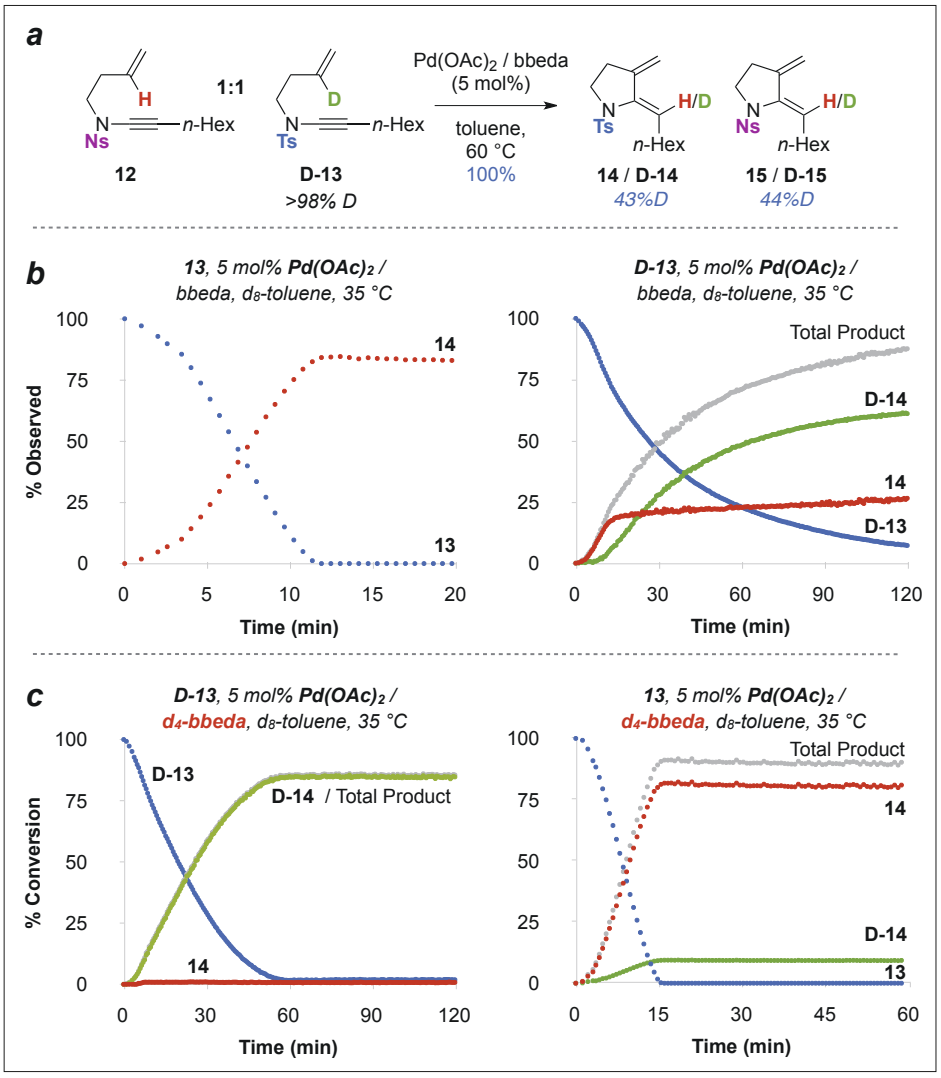

Scheme 5. Mechanistic observations: a) Crossover experiments; b) NMR reaction profiles of **13** and **D-13**; c) NMR reaction profiles using d_4-bbeda.

Rhodium-catalyzed Asymmetric [5+2] Cycloisomerization of Vinylcyclopropane Ynamides[13]

In this final example, computational investigations not only informed on an unexpected mechanistic pathway, but through the development of a robust transition state model enabled us to probe subtle electronic effects on reaction performance, and to influence ligand design. The subject of study was the [5+2] cycloisomerization[14] – a venerable transformation in the field thanks

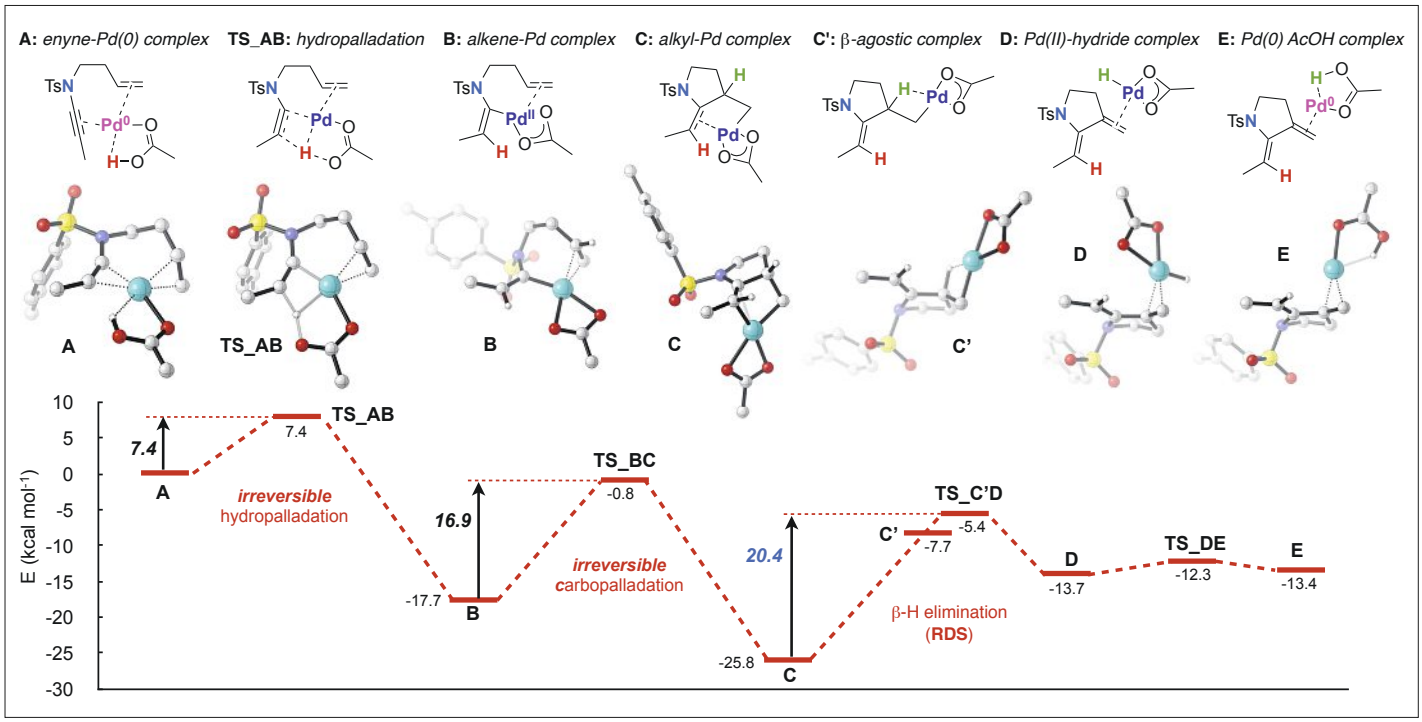

Scheme 6. Computational analysis of enynamide cycloisomerization.

to the extensive work of the Wender and Trost groups in establishing rhodium- and ruthenium-based catalysts systems, respectively. Continuing with our interests in ynamide chemistry, we recognized that the use of ynamide vinylcyclopropanes would provide an appealing entry to 5,7-fused azabicycles, especially if this chemistry could be realized asymmetrically. In that context, early work from Wender had demonstrated that rhodium-BINAP catalyst systems were capable of effecting asymmetric [5+2] processes;[15] however, it is the subsequent use of rhodium-phosphoramidite complexes by Hayashi and co-workers that resulted in a truly exceptional catalyst system.[15]

While our initial interests certainly lay in establishing whether vinylcyclopropane ynamides (**17**, Scheme 8) would be viable substrates in [5+2] chemistry, we became aware that in the general realm of asymmetric cycloisomerization, there were no successful examples of cycloisomerizations of chiral single enantiomer substrates with chiral catalysts in which the catalyst dominates the stereochemical outcome of the reaction in both the matched, and in particular the mismatched setting. This is a significant challenge in the general context of stereoselective synthesis, and we questioned whether ynamide vinylcyclopropanes could also provide a means to investigate catalyst-control over diastereoselective cycloisomerizations.

Initial investigations revealed rhodium catalysts to be highly efficient in mediating ynamide [5+2] cycloisomerization; in particular, the cationic rhodium-naphthalene complex **18** previously employed by Wender[16] translated smoothly to the ynamide setting, delivering azabicyclic products **19** in high yields and short reaction times (Scheme 8a). The effect of pre-existing stereocentres was clear from this work, with 5,7-azabicycles **19c**, **19d** and **19e** formed in up to 20:1 dr. These substrates revealed the powerful influence of the allylic stereocentre on reaction diastereoselectivity, and thus set a battleground for a chiral catalyst. In turn, a preliminary screen of various phosphoramidite ligands revealed that while respectable reactivity and selectivity was observed in several cases, the 'Feringa' phosphoramidite (**L1**, Scheme 8b)[17] was the most efficient and selective (giving **19f** in 15 min, 98% ee).

Curious to understand the source of enantioselectivity, we decided to subject this transformation to theoretical analysis. At the outset, we were mindful of the need to explore the two commonly accepted mechanisms for the [5+2] reaction (Scheme 9): a) the 'vinylcyclopropane' pathway, in which the metal initiates cycloisomerization by oxidative addition into the vinylcyclopropane allylic C–C bond (**F**→**G**), followed by migratory insertion of the tethered alkyne into the resultant 6-membered metallacycle, with reductive elimination from metallacycle **H** completing formation of the 7-membered ring; and b) the 'metallacyclopentene' pathway,

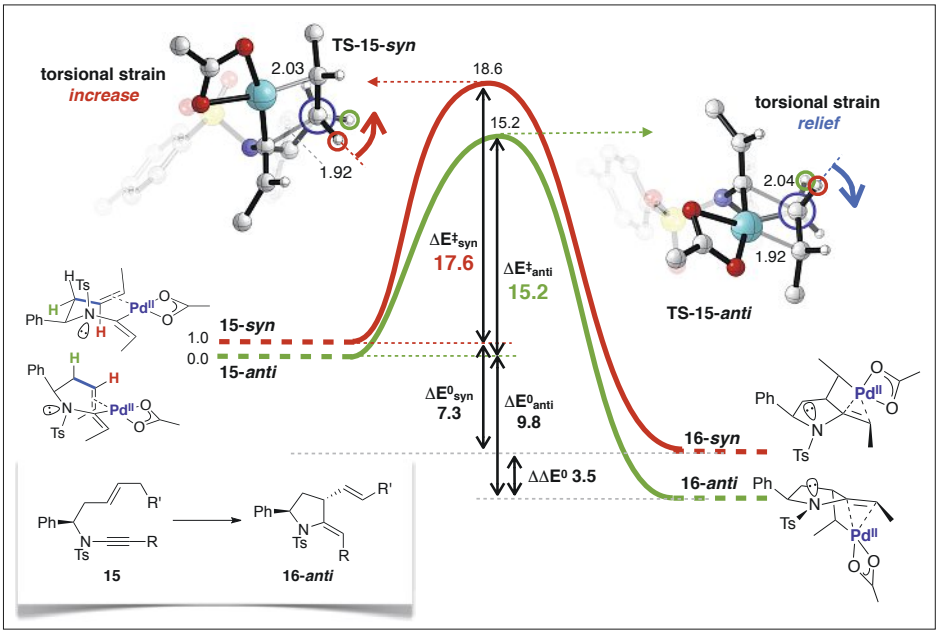

Scheme 7. Cycloisomerization diastereoselectivity derives from torsional strain effects.

whereby reaction initiation occurs through oxidative coupling of the metal-complexed enyne (**I**→**J**), followed by a ring expansion from the resultant rhodacyclopentene into the cyclopropane (affording the same 8-membered metallacycle **H** as in path a), and lastly reductive elimination. Previous work from the Houk group in collaboration with Wender has suggested that rhodium prefers to follow vinylcyclopropane path a),[18] while equivalent studies from the Houk and Trost groups support ruthenium catalysts favouring metallacyclopentene path b).[19]

We first considered the ground state complex formed between the vinylcyclopropane ynamide, and the rhodium-phosphoramidite complex. As for the Hayashi group's proposal of an empirical model for stereoinduction,[15b] we also took the rhodium-Feringa phosphoramidite-norbornadiene complex crystal structure (**20**, Scheme 10a), reported by Mezzetti and co-workers, as a starting point.[20] This structure shows the phosphoramidite to bind to the metal in a bidentate fashion, coordinated through phosphorous, and *via* η^2-complexation of one of the benzylic arenes. Imaginary decomplexation of norbornadiene thus affords a chiral metal ion environment to which an enyne – or enynamide – can coordinate. Computational screening of eight different orientations of the vinylcyclopropane enynamide on this metal centre was undertaken (enynamide oriented up/down, ynamide *trans* to the arene or phosphorous, and *Re/Si* face binding of the alkene), which revealed conformation **21** (Scheme 10b) to be the lowest energy ground state. Naturally, it is by no means certain that this lowest energy ground state should correlate with the lowest energy transition state of the reaction, and thus the two different reaction paths outlined in Scheme 9 were explored for each of the possible ground states. In the event, the lowest energy computed ground state indeed led to a lowest energy transition state **22** (Scheme 10c) – but to our surprise, the use of an ynamide in this chemistry leads to the unusual prediction of the metallacyclopentene pathway for this rhodium-catalyzed process, potentially due to the stronger binding of the electron rich ynamide alkyne to the metal centre compared to a regular alkyne.

This transition state and associated reaction profile provided the opportunity to probe the effects of adjusting the electronic profile of the ligand components on the *Re*/*Si* face energy barriers for this rate-limiting step, and hence to influence the predicted selectivity of the reaction. The benzylamine arm of the ligand is a particularly attractive place to do this, as this portion of the ligand can be easily varied experimentally by the synthesis of different amine components of the phosphoramidite, which derive from reductive amination of an α-methylbenzylamine derivative with the corresponding acetophenone. We elected to model two further ligands to explore this effect: **L2**, in which the arene is substituted at the *para* position with an electron-donating methoxy group, and **L3** in which it is fluorinated. The computational results were striking (Scheme 10d): a significant influence over the energy difference between the *Re* and *Si* face pathways was observed ($\Delta\Delta G^{\ddagger}$), leading to predicted enantioselectivities as shown. To our delight, these predicted values correlated extremely well with experiment. Equally significantly, this ligand also led to much enhanced rates of cycloisomerization (visualized theoretically through the relative heights of the activation barriers): ^{1}H NMR spectroscopic monitoring of ligands **L1**–**L3** revealed a remarkable trend in reactivity profile, with ligand **L3** leading to complete reaction in under five minutes, and in general enabling rapid and highly enantioselective [5+2] cycloisomerizations across a range of substrates. We believe the greater reactivity profile exhibited by this ligand relates to weaker complexation of the fluorobenzene to the metal,[21] in turn resulting in tighter binding of the substrate. This has two effects: first, to enhance the difference in energy between the *Re* and *Si* face pathways, leading to enhanced selectivity, and second, to progress the substrate further along the reaction coordinate by virtue of its stronger coordination to the metal centre.

With enantioselective reactions established, our attention finally turned to the challenging arena of diastereoselective reactions, and the prospect of achieving catalyst stereocontrol in both matched and mismatched settings (Scheme 11). In the former case, ligand **L3** maintained or enhanced reaction selectivity compared to substrate stereocontrol alone. Most pleasing, however, was that this ligand was also able to overturn substrate stereocontrol, delivering good levels of selectivity for the substrate disfavoured/catalyst favoured diastereomer (Scheme 11, mismatched). Interestingly, the 1:5 dr observed with **L3** for product **19g** proved not to be the best result in the mismatched reaction: the diastereoselectivity could be enhanced to 1:8 when using the non-fluorinated ligand **L1**, a seemingly paradoxical observation whereby ligands offering high enantioselectivity may not also deliver high diastereoselectivity in mismatched settings. This is a perhaps not unsurprising result if the reasons for the heightened reactivity of ligand **L3** are indeed based in tighter substrate binding, as in the present case this would increase the degree to which the reaction is 'mismatched' from the perspective of the substrate.

Conclusion

In conclusion, we hope this perspective highlights the insight and benefits that can be gained by the combined use of compu-

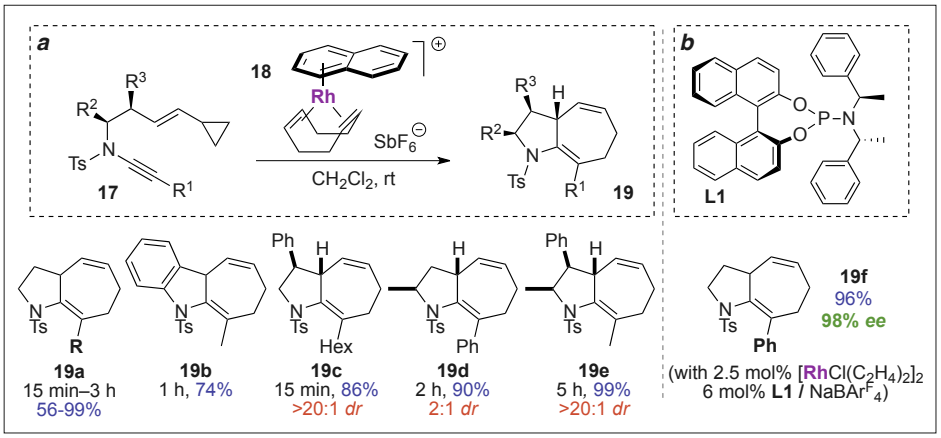

Scheme 8. a) Substrate stereocontrol in Rh-catalyzed ynamide [5+2] cycloisomerization. b) Preliminary asymmetric result.

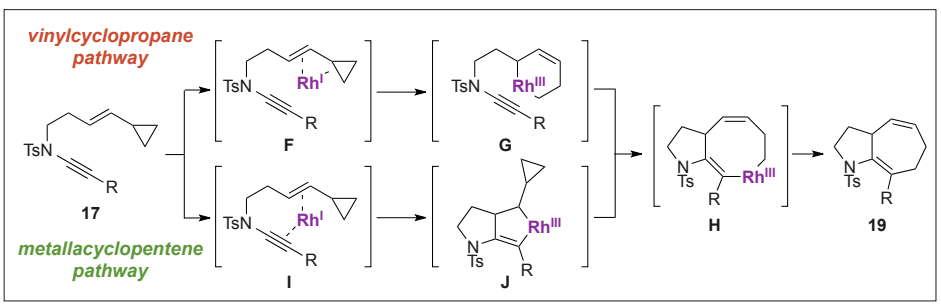

Scheme 9. Commonly accepted mechanisms for [5+2] cycloisomerization.

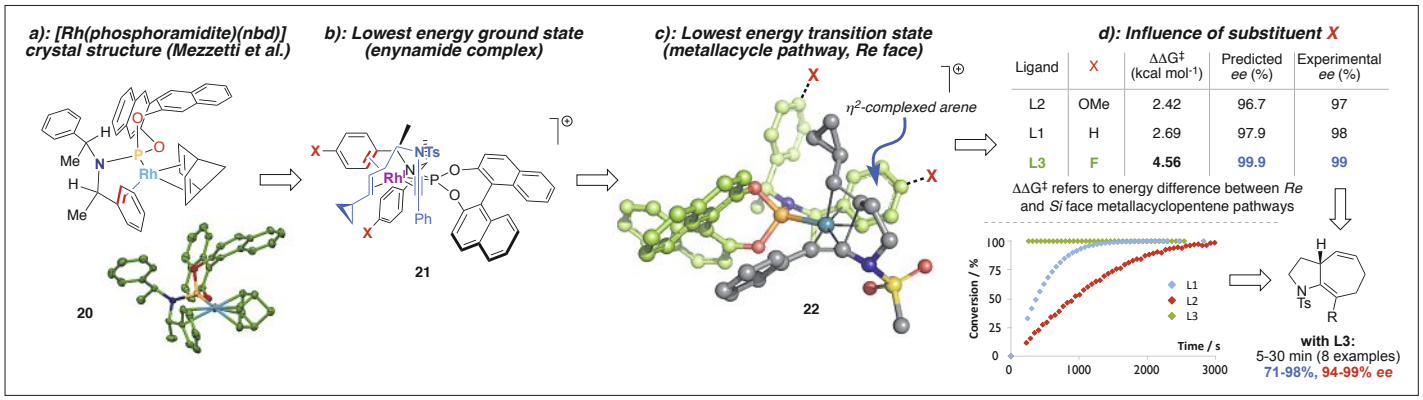

Scheme 10. Computational model for the cycloisomerization, and a combined theoretical and experimental approach to ligand design.

tational and experimental methods in developing and understanding catalytic processes. Reactivity, regioselectivity, enantioselectivity and diastereoselectivity are all susceptible to interrogation, and interpretation, using this synergistic approach. The modelling of increasingly ambitious and complex transformations is now a reality in modern chemistry; in this vein, our groups continue to explore new areas of catalysis and ligand design that can benefit from this approach.

Acknowledgements

EAA thanks the EPSRC (EP/E055273/1, EP/K005391/1, EP/H025839/1) for support for these projects. RSP thanks the Chemical Structure Association Trust and the use of the EPSRC UK National Service for Computational Chemistry Software (CHEM773).

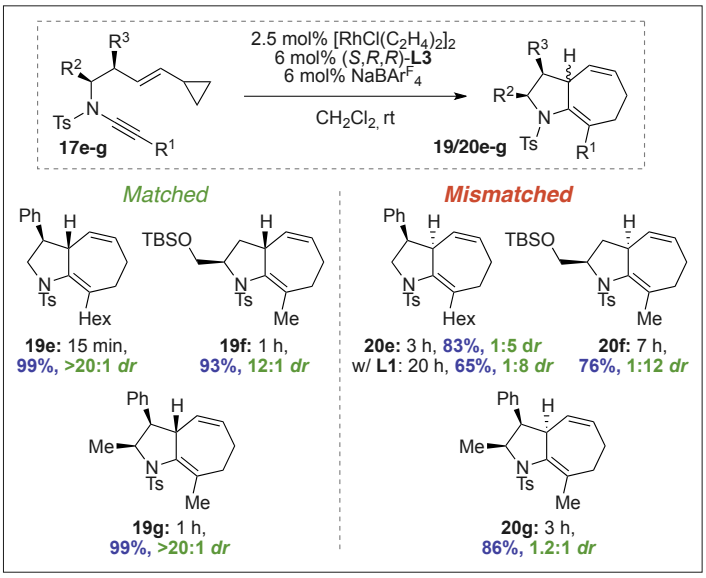

Scheme 11. Diastereoselective matched and mismatched catalyst/substrate stereocontrol.

Received: June 15, 2018

[1] V. Michelet, P. Y. Toullec, J. P. Genet, *Angew. Chem. Int. Ed.* **2008**, *47*, 4268.
[2] T. Sperger, I. A. Sanhueza, I. Kalvet, F. Schoenebeck, *Chem. Rev.* **2015**, *115*, 9532.
[3] a) D. S. B. Daniels, A. S. Jones, A. L. Thompson, R. S. Paton, E. A. Anderson, *Angew. Chem. Int. Ed.* **2014**, *53*, 1915; b) D. S. B. Daniels, A. L. Thompson, E. A. Anderson, *Angew. Chem. Int. Ed.* **2011**, *50*, 11506.
[4] C. J. Elsevier, H. Kleijn, J. Boersma, P. Vermeer, *Organometallics* **1986**, *5*, 716.
[5] P. W. N. M. van Leeuwen, P. C. J. Kamer, J. N. H. Reek, P. Dierkes, *Chem. Rev.* **2000**, *100*, 2741.
[6] a) J. Tsuji, T. Mandai, *Angew. Chem. Int. Ed.* **1995**, *34*, 2589; b) L. N. Guo, X. H. Duan, Y. M. Liang, *Acc. Chem. Res.* **2011**, *44*, 111; c) For a review of Pd-catalyzed cascade processes, see: T. Vlaar, E. Ruijter, R. V. A. Orru, *Adv. Synth. Catal.* **2011**, *353*, 809; d) V. Franckevičius, *Tetrahedron Lett.* **2016**, *57*, 3586.
[7] A. Wojcicki, *Inorg. Chem. Commun.* **2002**, *5*, 82.
[8] S. Ogoshi, K. Tsutsumi, H. Kurosawa, *J. Organomet. Chem.* **1995**, *493*, C19.
[9] A. Mekareeya, P. R. Walker, A. Couce-Rios, C. D. Campbell, A. Steven, R. S. Paton, E. A. Anderson, *J. Am. Chem. Soc.* **2017**, *139*, 10104.
[10] B. M. Trost, M. Lautens, *J. Am. Chem. Soc.* **1985**, *107*, 1781.
[11] a) For seminal work on enynes, see: B. M. Trost, G. J. Tanoury, M. Lautens, C. Chan, D. T. Macpherson, *J. Am. Chem. Soc.* **1994**, *116*, 4255; b) B. M. Trost, D. L. Romero, F. Rise, *J. Am. Chem. Soc.* **1994**, *116*, 4268; c) B. M. Trost, *Acc. Chem. Res.* **1990**, *23*, 34.
[12] a) R. L. Greenaway, C. D. Campbell, O. T. Holton, C. A. Russell, E. A. Anderson, *Chem. Eur. J.* **2011**, *17*, 14366; b) R. L. Greenaway, C. D. Campbell, H. A. Chapman, E. A. Anderson, *Adv. Synth. Catal.* **2012**, *354*, 3187; c) P. R. Walker, C. D. Campbell, A. Suleman, G. Carr, E. A. Anderson, *Angew. Chem. Int. Ed.* **2013**, *52*, 9139; d) For related Diels-Alder reactions of exocyclic 2-amidodienes, see: C. D. Campbell, R. L. Greenaway, O. T. Holton, P. R. Walker, H. A. Chapman, C. A. Russell, G. Carr, A. L. Thomson, E. A. Anderson, *Chem. Eur. J.* **2015**, *21*, 12627; e) For reviews, see: X.-N. Wang, H.-S. Yeom, L.-C. Fang, S. He, Z.-X. Ma, B. L. Kedrowski, R. P. Hsung, *Acc. Chem. Res.* **2013**, *47*, 560.
[13] R. N. Straker, Q. Peng, A. Mekareeya, R. S. Paton, E. A. Anderson, *Nat. Commun.* **2016**, *7*, 10109.
[14] a) K. E. O. Ylijoki, J. M. Stryker, *Chem. Rev.* **2013**, *113*, 2244; b) H. Pellissier, *Adv. Synth. Catal.* **2017**, *360*, 1551.
[15] a) More modest enantioselectivities have been observed using Rh-BINAP complexes. See: P. A. Wender, L. O. Haustedt, J. Lim, J. A. Love, T. J. Williams, J.-Y. Yoon, *J. Am. Chem. Soc.* **2006**, *128*, 6302; b) R. Shintani, H. Nakatsu, K. Takatsu, T. Hayashi, *Chem. Eur. J.* **2009**, *15*, 8692.
[16] P. A. Wender, T. J. Williams, *Angew. Chem. Int. Ed.* **2002**, *41*, 4550.
[17] J. F. Teichert, B. L. Feringa, *Angew. Chem. Int. Ed.* **2010**, *49*, 2486.
[18] a) X. Xu, P. Liu, A. Lesser, L. E. Sirois, P. A. Wender, K. N. Houk, *J. Am. Chem. Soc.* **2012**, *134*, 11012; b) P. Liu, L. E. Sirois, P. H.-Y. Cheong, Z.-X. Yu, I. V. Hartung, H. Rieck, P. A. Wender, K. N. Houk, *J. Am. Chem. Soc.* **2010**, *132*, 10127.
[19] X. Hong, B. M. Trost, K. N. Houk, *J. Am. Chem. Soc.* **2013**, *135*, 6588.
[20] I. S. Mikhel, H. Ruegger, P. Butti, F. Camponovo, D. Huber, A. Mezzetti, *Organometallics* **2008**, *27*, 2937.
[21] S. D. Pike, I. Pernik, R. Theron, J. S. McIndoe, A. S. Weller, *J. Organomet. Chem.* **2015**, *784*, 75.